JOURNAL OF GEOPHYSICAL RESEARCH, VOL. 99, NO. B7, PAGES 13,913–13,921, JULY 10, 1994

Valley incision and the uplift of mountain peaks

David R. Montgomery

Department of Geological Sciences and Quaternary Research Center, University of Washington, Seattle

Abstract. Simple end-member models describe the effect of isostatically compensated valley incision on the elevation of mountain peaks. These models allow calculation of the maximum portion of mountain peak elevations attributable to the development of observed relief and predict general downstream patterns of ridgetop uplift in response to erosion by fluvial processes. Analyses of topographic profiles across major drainages of the central Sierra Nevada and the Tibetan Plateau indicate that isostatically compensated valley incision could account for at most 5–10% of the present elevation of mountain peaks. In contrast, analyses of topographic profiles across the Himalaya show that as much as 20–30% of the present elevation of Himalayan peaks could be explained by isostatically compensated valley incision. The degree to which valley incision is compensated locally, however, depends on the flexural rigidity of the lithosphere, the size of the range, and its tectonic boundary conditions. These results show that while a tectonic control is required for late Cenozoic surface uplift of the Sierra Nevada, a significant portion of the elevation of Himalayan peaks may reflect late Cenozoic valley incision on the margin of the Tibetan Plateau.

Introduction

The potential for raising mountain peaks in response to isostatically compensated deepening of valleys has been recognized for many years [e.g., *Nansen*, 1928; *Wager*, 1933, 1937; *Holmes*, 1945]. *Molnar and England* [1990], however, recently proposed that accelerated valley erosion resulting from climate change could explain a variety of evidence for late Cenozoic surface uplift from many of the world's mountain ranges. They suggested that much of the geologic evidence for accelerated "uplift" does not necessarily record surface uplift but rather records accelerated erosion and bedrock unroofing. They further offered the hypothesis that late Cenozoic climate change increased valley incision and induced uplift of mountain peaks as an alternative to the hypothesis that tectonically controlled uplift triggered onset of the Quaternary ice ages (see review by *Raymo and Ruddiman* [1992]). These hypotheses may be explored using existing relief to constrain the potential influence of valley incision on the elevation of mountain peaks. This paper develops a model of this relation, estimates the total uplift of mountain peaks attributable to valley incision for the central Sierra Nevada and the Nepalese Himalaya, explores a model for general patterns of downstream ridgetop uplift in response to fluvial erosion, and discusses the influence of mountain range scale and lithosphere strength on the isostatic response to valley incision.

Isostatic Response to Valley Incision

As valleys enlarge, isostatic rebound increases the elevation of mountain peaks or unincised portions of an original surface (Figure 1). A simple relation between valley incision and the resulting uplift of mountain peaks may be formalized by adopting the limiting assumptions of local isostatic compensation and a two-dimensional geometry. The resulting model illustrates general controls on the potential influence of valley deepening on the elevation of mountain peaks.

Paper number 94JB00122.
0148-0227/94/94JB-00122$05.00

Model

The spatially averaged erosion rate (E) for incision of periodic topography (Figure 2a) with a spatially uniform relief (R) between the elevation of mountain peaks (Z_p) and valley bottoms (Z_v) is given by

$$E = (1/2)dZ_v/dt \quad (1)$$

where dZ_v/dt is the rate of valley incision relative to the elevation of bounding peaks. Bedrock strength properties, however, may impose limits to local relief development [*Schmidt and Montgomery*, 1992]. This formulation also assumes that valley sides steepen as a valley deepens, implying that broad valley floors do not develop, a reasonable assumption within many mountain environments where floodplain rivers are uncommon.

The rebound rate, and thus the uplift rate of mountain peaks (dZ_p/dt), from local isostatic compensation is

$$dZ_p/dt = (1/2)(\rho_c/\rho_m)dZ_v/dt, \quad (2)$$

where ρ_c is the density of the crust and ρ_m is the density of the mantle. The uplift rate of mountain peaks is thus a fraction of the valley incision rate. Assuming crust and mantle densities of 2800 and 3300 kg/m^3, respectively, implies that the rate of elevation increase for mountain peaks will be 42% of the rate of valley incision. This means that excavation of very deep valleys is necessary to significantly raise mountain peaks by this mechanism.

In the corresponding model for uplift of a partially incised surface (Figure 2b), the proportion of the original surface remaining undissected influences the spatially averaged erosion rate and thus the rebound rate. For the geometry illustrated in Figure 2b, the spatially averaged erosion rate resulting from valley incision is

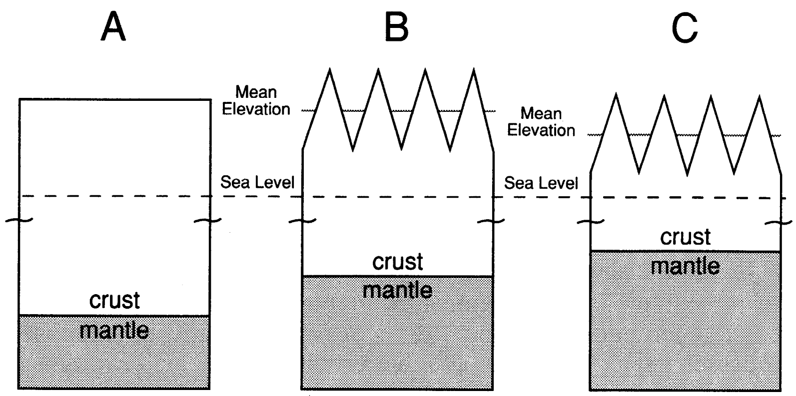

Figure 1. Illustration of the isostatic uplift of mountain peaks in response to valley incision. (a) Erosion of deep valleys in an initially level plateau leads to (b) a landscape with a lower mean elevation with mountain peaks rising above the elevation of the original plateau. (c) Erosion that does not increase relief lowers both the mean elevation and mountain peaks.

$$E = (1/2)[V/(V + P)](dZ_v/dt), \quad (3)$$

where V is the valley width and P is the width of the unincised surface between valleys. The rate of isostatically compensated peak uplift of a plateau surface is then

$$dZ_p/dt = (1/2)[V/(V + P)](\rho_c/\rho_m)(dZ_v/dt). \quad (4)$$

Thus the uplift rate of unincised portions of an initial surface is related to both valley spacing and the rate of valley incision.

A more general model for elevation of mountain peaks in response to valley incision applies to variably incised landscapes (Figure 3). For a cross section of unit width, the spatially averaged thickness of eroded material (D_e) is equal to

$$D_e = A_e/W, \quad (5)$$

where A_e is the area of material eroded from the cross section and W is the width of the cross section. The total uplift of peaks attributable to isostatically-compensated erosion (ΔZ_p) is then

$$\Delta Z_p = (A_e/W)(\rho_c/\rho_m). \quad (6)$$

(Note that (6) is not subject to the assumption that valley sides steepen as a valley deepens.) In this manner, the area of material eroded from below mountain peaks in a topographic cross section constrains the total uplift of the peaks that is potentially attributable to valley incision.

The assumption of local isostatic compensation has a substantial influence on the applicability of the model, as will be discussed in more detail, because flexural rigidity of the lithosphere reduces the degree of local isostatic compensation [e.g., *Banks et al.*, 1977]. Consequently, this model predicts the maximum potential uplift of mountain peaks by this mechanism. The model is two-dimensional, however,

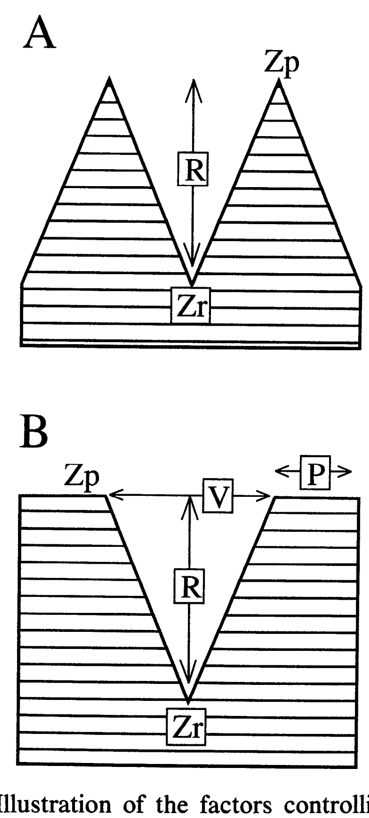

Figure 2. Illustration of the factors controlling mountain peak uplift in response to valley incision for (a) periodically dissected topography and (b) a partially dissected plateau surface.

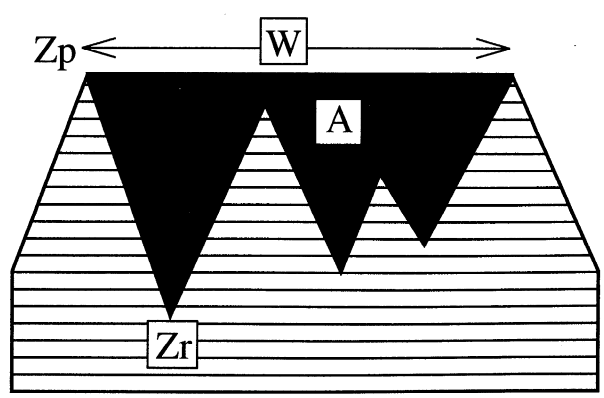

Figure 3. Illustration of topographic cross section across a mountain range showing material eroded from elevations below the peaks (solid area).

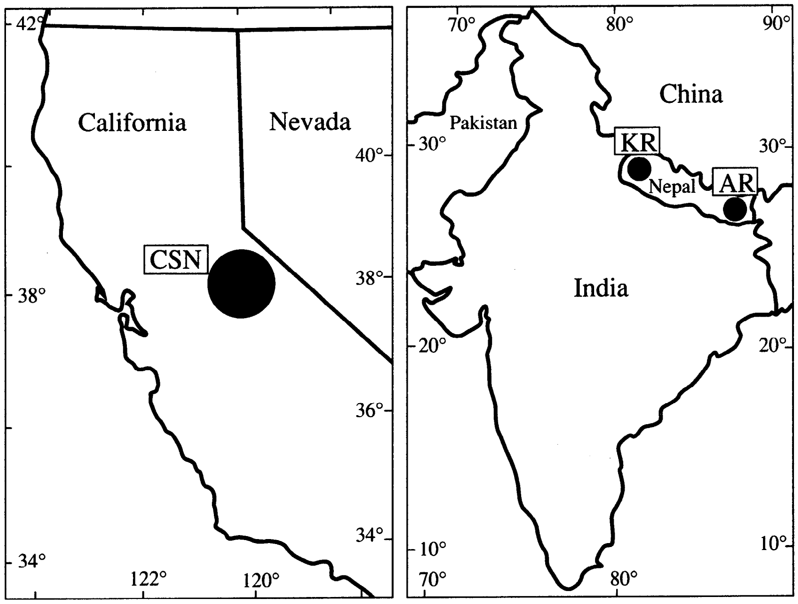

Figure 4. Maps showing locations of (a) central Sierra Nevada (CSN) and (b) the Karnali (KR) and Arn (AR) Rivers in the Nepalese Himalaya.

and essentially simulates uplift resulting from incision of long parallel valleys; dissection by a grid of orthogonally oriented valleys would result in greater elevation of mountain peaks. Thus these assumptions are partially offsetting.

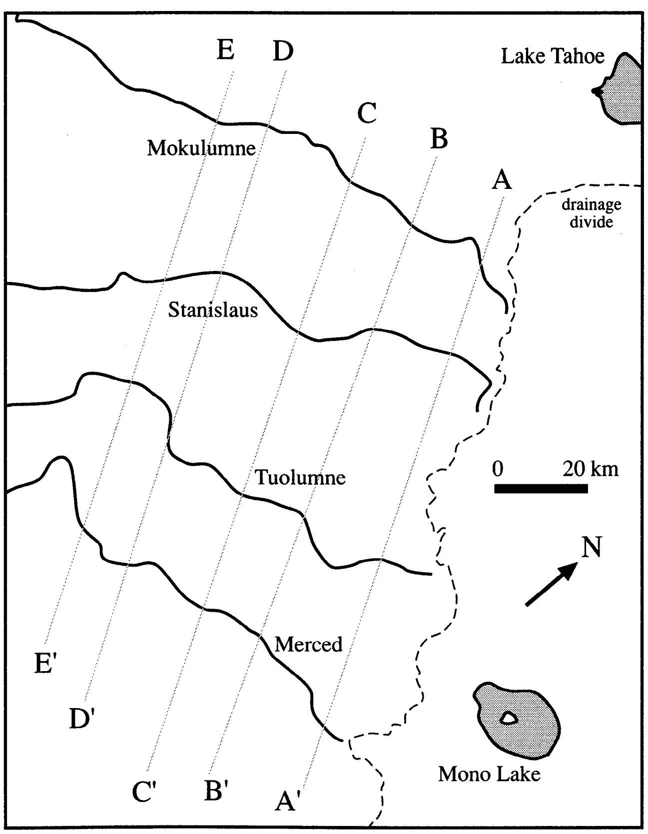

Figure 5. Map showing the location of major drainages in the central Sierra Nevada and topographic cross sections shown in Figure 6.

The predicted uplift of mountain peaks by this mechanism is explored below for the central Sierra Nevada and the Nepalese Himalaya (Figure 4).

Sierra Nevada

A variety of stratigraphical, geomorphological, and paleobotanical evidence have been interpreted as suggesting that uplift of the Sierra Nevada started roughly 10 Ma and accelerated sometime between 3 and 5 Ma [e.g., *Le Conte*, 1886; *Mathes*, 1930; *Axelrod*, 1957; *Hudson*, 1960; *Christensen*, 1966; *Huber*, 1981; *Unruh*, 1991]. Although broad uplands between the major drainages of the Sierra Nevada have been interpreted by some as an incised erosion surface [*Mathes*, 1930], *Wahrhaftig* [1965] argued that these surfaces reflect weathering-limited erosion. In either case, the deeply incised valleys of the central Sierra Nevada provide an opportunity to examine the possible influence of valley incision on uplift of the range.

Topographic profiles across four major drainages in the central Sierra Nevada (Figure 5) were generated from the U.S. Geological Survey 1:500,000 topographic map of California, and elevations of mountain peaks were connected to define a reference surface for calculating valley incision (Figure 6). Although the original surface may have been higher than that reconstructed from the elevation of contemporary peaks, the degree of incision below peaks effectively constrains the total uplift of mountain peaks attributable to valley incision, as opposed to other hypothesized tectonic mechanisms for uplift of the Sierra Nevada [e.g., *Chase and Wallace*, 1986].

Assuming that incision of the valleys occurred after 10 Ma, the cross-sectional area of material eroded from below the surface defined by mountain peaks provides long-term average erosion rate estimates of roughly 0.01 to 0.02 mm/yr (Table 1). Total surface uplift attributable to valley incision determined using (6) varies from about 200 m in the high

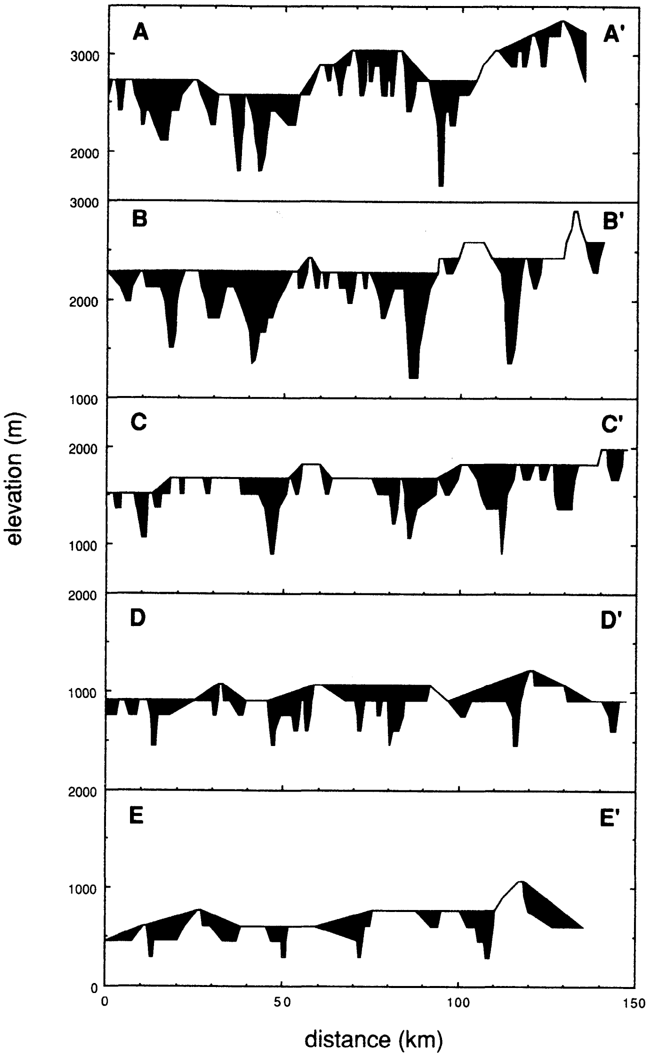

Figure 6. Topographic cross sections across the central Sierra Nevada; shaded area shows difference between present topography and approximate 10 Ma surface reconstructed from peak elevations.

Sierra to less than 100 m at the western edge of the Sierra foothills, of the order of 5–10% of the present elevation of the range. *Huber* [1990] estimated as much as 1830 m of post-10 Ma uplift in the headwaters of the Tuolumne river. The calculated uplift for locally compensated valley incision of about 172 m from the corresponding cross section (A-A′ in Figure 6) would account for only 9% of Huber's uplift estimate, implying that a tectonic mechanism is required to explain uplift of the Sierra Nevada.

Himalaya

The Himalaya occupies the edge of the Tibetan Plateau, which was uplifted in response to the collision of the Indian and Asian plates [*Molnar and Tapponnier*, 1975]. While much of the available evidence indicates uplift of the Tibetan Plateau to its present elevation by the end of the Miocene [*Mercier et al.*, 1987; *Harrison et al.*, 1992; *Pan and Kidd*, 1992], there are conflicting reconstructions for the uplift history of Himalayan peaks [e.g., *Cervany et al.*, 1988; *Copeland and Harrison*, 1990; *Amano and Tiara*, 1992]. Several workers, however, have suggested that the great height of Himalayan peaks results from incision of trans-Himalayan valleys [*Wager*, 1933, 1937; *Bird*, 1978]. While estimation of the mass eroded from beneath existing Himalayan peaks cannot address uplift timing, it can establish how much of their present elevation potentially could be attributed to increased late Cenozoic valley erosion.

Topographic profiles across the Karnali River and the western third of Nepal (Figure 7) allow a preliminary estimate of the potential uplift of Himalayan peaks resulting from valley incision. Three profiles crossing the Himalaya and two crossing the headwaters of the river in the Tibetan Plateau were generated from the Defense Mapping Agency 1:1,000,000 scale Operational Navigation Chart ONC H-9 (Figure 8). The greatest relief in the Himalaya is on the edge of the Tibetan Plateau, where the Karnali River is incised up to 4500 m below the surrounding peaks. Relief in both the Tibetan Plateau and lower Himalaya is of the order of 1000 m. Incorporating the area of material inferred to have been eroded from between peak elevations and the present topography into (6) implies that 500 m of summit uplift (roughly 9% of the present elevation) is potentially attributable to isostatically compensated valley incision in the Tibetan Plateau but that almost 1500 m of uplift of Himalayan peaks could be attributable to this mechanism (Table 2). Thus as much as 20–30% of the present elevation of Himalayan peaks could be attributed to valley incision.

A simple test of whether incision of trans-Himalayan valleys could have occurred in response to late Cenozoic climatic change is given by average erosion rates derived by assuming that all of the erosion implied in Figure 8 occurred since 3 Ma. Post-Miocene average erosion rates in the Nepalese Himalaya of 1.2 mm/yr [*Hubbard et al.*, 1991] are significantly greater than the erosion rates of 0.2–0.6 mm/yr

Table 1. Sierra Nevada

Cross Section	Elevation, m	Average Erosion, m	Peak Rebound, m	Percent*	Erosion Rate,† mm/yr
A-A′	2800	205	172	6	0.021
B-B′	2350	209	176	7	0.021
C-C′	1675	124	104	6	0.012
D-D′	900	88	74	8	0.009
E-E′	670	82	69	10	0.008

*Peak rebound/elevation.
†Average erosion rate required for all erosion to postdate 10 Ma.

required under this limiting assumption (Table 2). While this does not confirm that significant uplift of Himalayan peaks reflects a late Cenozoic increase in valley incision, especially since river valleys must have crossed the Himalaya prior to 3 Ma, it does indicate that significant uplift of Himalayan peaks could have occurred in response to a late Cenozoic acceleration of valley incision.

Downstream Surface Uplift From Fluvial Incision

Under the limiting assumption of local isostatic compensation, downstream variations in valley incision imply general downstream patterns of ridge top profiles. Erosion of valleys occurs over long time scales by fluvial incision, knickpoint propagation, glacial scour, and incision by debris flows. Transport laws (formal expressions for the controls on rates of erosion) have been proposed for a variety of processes [e.g., *Kirkby*, 1971], but of the processes contributing to valley incision, transport laws for erosion by fluvial processes have the strongest theoretical basis. Thus I will consider only valley incision by fluvial processes, even though debris flow processes may dominate sediment transport and river profile development in steep mountain channels [*Seidl and Dietrich*, 1992].

A simple mechanistic erosion law for fluvial incision assumes that erosion is proportional to stream power, which is proportional to the product of water discharge Q and local valley slope dZ_v/dx:

$$dZ_v/dt = k_1 Q(dZ_v/dx) \qquad (7)$$

where k_1 is a constant. Discharge, in turn, is proportional to drainage area A:

$$Q = k_2 A^n, \qquad (8)$$

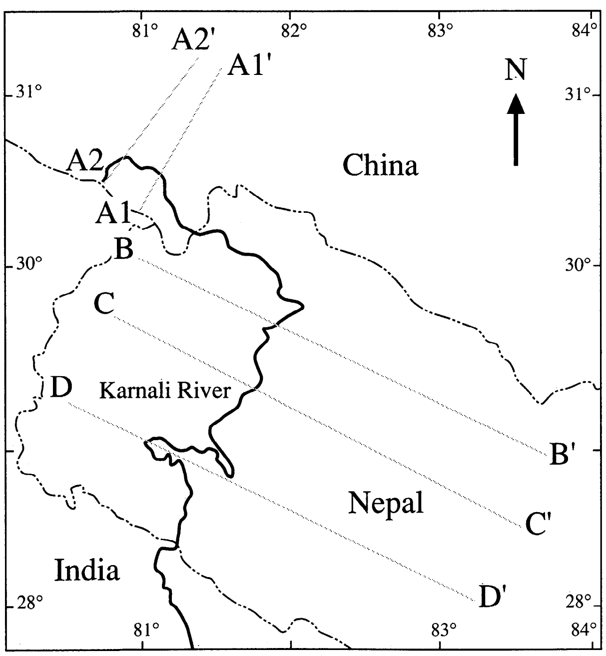

Figure 7. Map of the western Nepal showing location of topographic cross sections and river profiles shown in Figures 8 and 11.

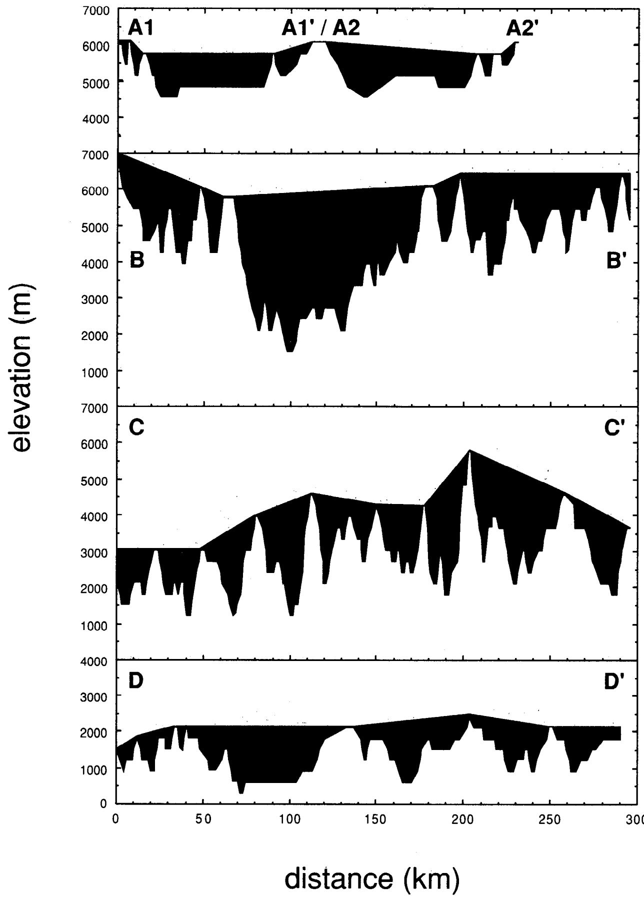

Figure 8. Topographic cross sections across the Himalaya in the Karnali River area; shaded area shows difference between present topography and approximate surface reconstructed from peak elevations.

where n is an exponent that for bankfull discharge varies regionally from about 0.7 to almost 1.0 and in many areas is essentially 1.0 for average annual discharge [*Dunne and Leopold*, 1978]. Drainage area is a function of the catchment length, or the distance from the drainage divide (x), and empirical data from the full range of natural drainage basin sizes are well-described by

$$A = x^2/3 \qquad (9)$$

[*Montgomery and Dietrich*, 1992]. Substituting (9) into (8) and the result (assuming $n = 1.0$) into (7) yields an erosion law formulated as

$$dZ_v/dt = kx^2(dZ_v/dx) \qquad (10)$$

where $k = k_1 k_2/3$. The corresponding isostatically compensated peak uplift rate is

$$dZ_p/dt = (1/2)k(\rho_c/\rho_m)x^2(dZ_v/dx). \qquad (11)$$

The evolution of river and mountain peak profiles were simulated using (10) and (11) for boundary conditions approximating those for the Sierra Nevada and Himalaya. Slope differences (dZ_v/dx) between successive river nodes were used in (10) and (11) to iteratively calculate changes in valley bottom and ridge top elevations at the downstream node for each time step.

Table 2. Himalaya

Cross Section	Elevation, m	Average Erosion, m	Peak Rebound, m	Percent*	Erosion Rate,† mm/yr
A-A′	5780	638	536	9%	0.213
B-B′	6230	1765	1482	24%	0.588
C-C′	4250	1300	1092	26%	0.433
D-D′	2130	766	643	30%	0.255

*Peak rebound/elevation.
†Average erosion rate required for all erosion to postdate 3 Ma.

Inclined Block

General downstream patterns of predicted valley incision and ridgetop uplift for the Sierra Nevada were simulated with an initial condition of an inclined block. The modeled region consisted of an inclined 120-km-long plane with a maximum elevation of 3 km and an elevation of 0 km at the basin outlet (Figure 9a). The surface was assumed to be initially unincised ($Z_p = Z_v$). While these assumptions and constraints would not be true in a natural landscape, one may visualize the model as simulating the change in valley and ridge profiles from an initial configuration in response to locally compensated valley incision.

Evolution of river and peak elevations was simulated at 5 km intervals along the profile for a period of 10 m.y. using (10) and (11) with 0.25-m.y. time steps, $k = 0.5$ m^{-1} yr^{-1}, and $\rho_c/\rho_m = 0.84$. Calculated profiles show that fluvial incision and predicted peak uplift is greatest in the lower portions of the simulated mountain range. River and peak profiles for the major drainages of the central Sierra Nevada (Figure 10), however, indicate that the greatest relief between ridge top and river elevations occurs in the upper portions of the drainages. Moreover, there are steps in the Tuolumne and Merced long profiles where glaciers gouged steps in the river long profile [e.g., *Cotton*, 1941]. Inclusion of an elevation dependence in the erosion law could provide a better fit between predicted and observed profiles and would be more consistent with a glacial mechanism for valley incision but still would not account for steps in the long profile.

Plateau Edge

Downstream patterns of river incision and ridgetop uplift in the Himalaya were modeled by incision of a plateau edge. The modeled region consists of a 250-km-wide plateau at an elevation of 6 km that drops to a local base level (0-km elevation) at a distance of 300 km from the drainage divide (Figure 9b). Again, the initial condition was an unincised surface.

Evolution of river and peak elevations was simulated at 5-km intervals along the profile for a period of 3 Ma using

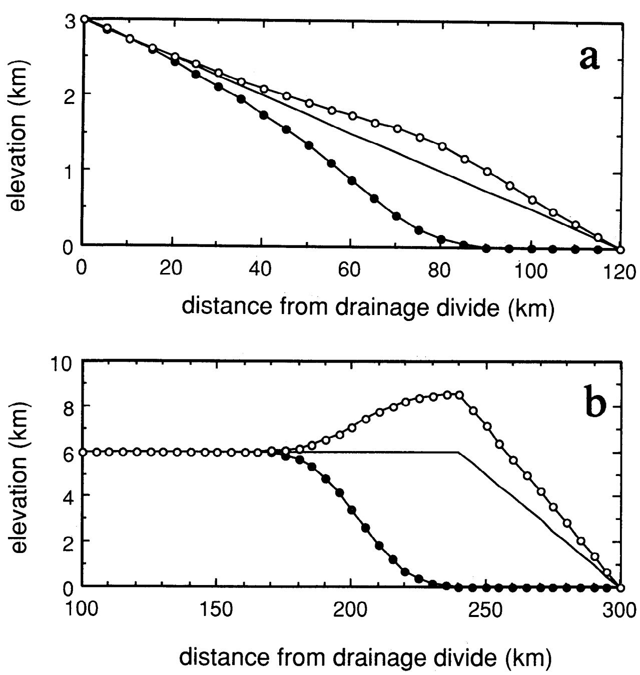

Figure 9. Simulated summit (open circles) and river (solid circles) profiles generated using equations (10) and (11) for incision of (a) an inclined block ($k = 0.5$ m^{-1} yr^{-1}, $t = 10$ Ma) and (b) plateau edge ($k = 0.4$ m^{-1} yr^{-1}, $t = 3$ Ma). Lines without data points represent initial condition.

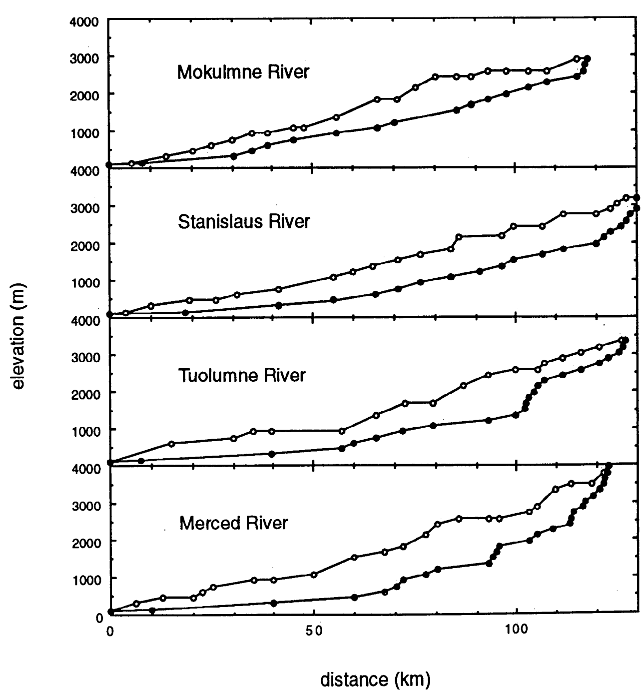

Figure 10. Long profiles of mountain peak (open circles) and river (solid circles) elevations for major drainages of the central Sierra Nevada.

(10) and (11) with 0.10-m.y. time steps, $k = 0.4\ \mathrm{m}^{-1}\ \mathrm{yr}^{-1}$, and $\rho_c/\rho_m = 0.84$. Calculated profiles show significant uplift of mountain peaks at the edge of the original plateau and a decreasing relief downstream, in contrast to the pattern predicted for incision of an inclined block (Figure 9a). Rivers crossing the Nepalese Himalaya (Figure 11) exhibit general patterns of mountain peak elevations and river profiles similar to model predictions. Again, however, incision by glacial mechanisms in the basin headwaters may control the pattern of river incision and peak uplift in the highest elevations. In either case, the downstream pattern of river and peak elevations strongly supports the hypothesis that the great height of Himalayan peaks is due to incision of the edge of the Tibetan Plateau.

Discussion

The approach employed above is limited by application of a two-dimensional analysis to a three-dimensional problem and assumption of local isostatic compensation. Although a grid of valleys would result in greater net uplift of mountain peaks, the basic approach illustrates constraints on the uplift of mountain peaks in response to valley erosion. Analysis of wide bands of topography using digital elevation models would more rigorously address the magnitude of peak uplift attributable to isostatically compensated valley incision, but such an analysis is not expected to yield substantially different results.

The flexural rigidity of the lithosphere, on the other hand, can have a great effect on the degree of local isostatic compensation. The percent of local isostatic compensation (C) that will be realized for periodic topography is a function of the density contrast between the crust and mantle, the flexural rigidity of the lithosphere (D), and the wavelength of the topography (λ):

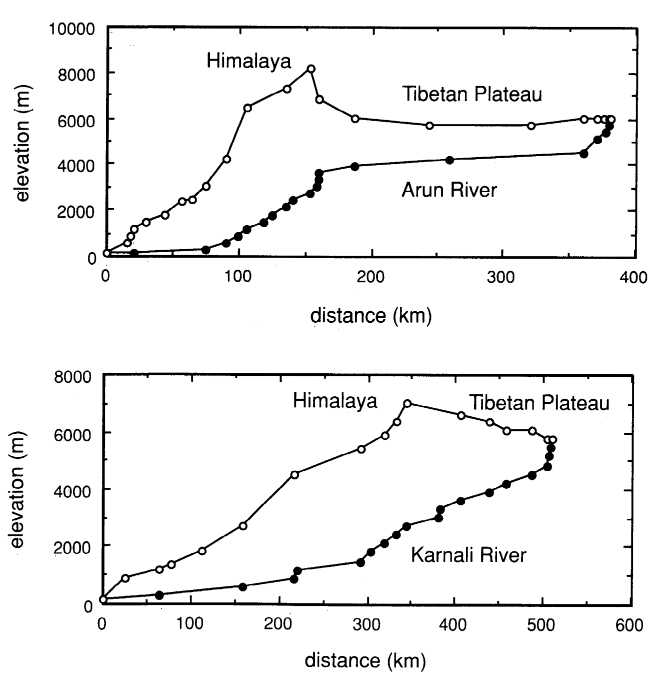

Figure 11. Long profiles of mountain peak (open circles) and river (solid circles) elevations for the Karnali and Arun Rivers from the Tibetan Plateau across the Himalaya.

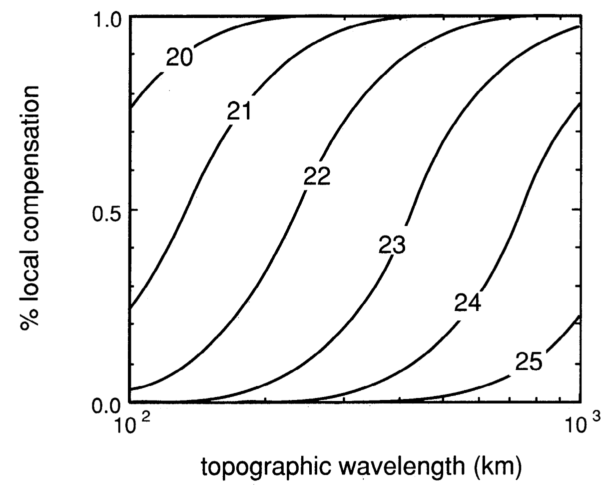

Figure 12. Solutions of equation (12) showing the predicted normalized percent of local isostatic compensation as a function of topographic wavelength and the flexural rigidity of the lothosphere. Contours are the exponent for flexural rigidity across a range of 10^{20} to 10^{25} N m.

$$C = (\rho_m - \rho_c)/[\rho_m - \rho_c + (D/g)(2\pi/\lambda)^4] \qquad (12)$$

where g is gravitational acceleration [*Turcotte and Schubert*, 1982]. Solutions of (12) for a range of topographic wavelengths (10^2–10^3 km) encompassing the width of most mountain ranges and a range of flexural rigidities (10^{20}–10^{25} N m) spanning those calculated for many regions [e.g., *Walcott*, 1970; *McNutt and Menard*, 1978; *Stephenson*, 1984; *Forsyth*, 1985] illustrate the range of conditions under which local isostatic compensation may be significant (Figure 12). Tectonic boundary conditions, however, also influence the degree to which local isostatic compensation may occur. A number of workers, for example, have discussed the influence of rift margins on local uplift [e.g., *Weissel and Karner*, 1989; *Gilchrist and Summerfield*, 1990; *ten Brink and Stern*, 1992]. The degree of local compensation thus is a function of the thickness and strength of the lithosphere and of the size and tectonic boundary conditions of the mountain range.

Estimates of the flexural rigidity and the wavelength of the Sierra Nevada and Himalaya can be used in (12) to estimate the degree to which valley incision is locally compensated in each range. *Chase and Wallace* [1986] estimate that the flexural rigidity of the lithosphere beneath the roughly 100- to 200-km-wide Sierra Nevada is of the order of 10^{23} to 10^{24} N m. For these conditions, (12) predicts of the order of only 1–5% local compensation. The faulted east side of the Sierra Nevada, however, is akin to a broken plate margin which will increase the degree of local compensation. In contrast, *Lyon-Caen and Molnar* [1983] estimated a flexural rigidity of 10^{22} to 10^{23} N m beneath the approximately 400- to 500-km-wide Himalaya. This implies isostatic compensation of the order of 45–95% of local compensation. Figure 12 further illustrates the scale dependence to the influence of valley incision on the elevation of mountain peaks. Even a low flexural rigidity is sufficient to suppress local compensation at topographic wavelengths less than about 100 km. Thus small-scale valley development will not influence mountain peak elevations. Valley incision is most effective at influencing the elevation of mountain peaks in either large mountain ranges or areas with a thin or weak lithosphere.

Conclusions

Incision of very deep valleys in large mountain ranges is required to generate significant uplift of mountain peaks from erosional mechanisms. Little is known, however, about rates of river incision into bedrock (see discussion by *Seidl and Dietrich* [1992]) and a greater understanding of the time required for river profile development in mountain drainage basins is necessary to better address the effect of valley incision on late Cenozoic mountain uplift. The results presented above, however, confirm that a tectonic mechanism is necessary to explain late Cenozoic surface uplift of the Sierra Nevada. For the Himalaya, on the other hand, isostatically compensated valley incision may account for as much as 1500 m of the elevation of mountain peaks, implying that increased late Cenozoic valley erosion may explain a significant portion of the great height of Himalayan peaks. Moreover, spatial patterns of peak and river elevations are consistent with the hypothesis that uplift of the Himalaya is a result of incision of the edge of the Tibetan Plateau.

An increase in relief is required to increase the elevation of mountain peaks through erosional mechanisms, such as those that might accompany climate change. An increase in erosion that does not influence relative erosion rates between valleys and ridges will simply result in accelerated denudation of the entire landscape. Controls on the spatial variability of erosional processes are thus fundamental to understanding the potential influence of climate change on the uplift of mountain peaks.

Notation

- A drainage area, m^2.
- A_e area eroded from cross section, m^2.
- D flexural rigidity of the lithosphere, N m.
- D_e average depth of erosion, m.
- E average erosion rate, m/yr.
- g gravitational acceleration, m/s^2.
- k proportionality constant, m^{-1} yr^{-1}.
- P undissected plateau width, m.
- Q river discharge, m^3/s.
- R relief between peak and valley bottom elevations, m.
- t time, Ma.
- V valley width, m.
- W cross section width, m.
- x distance from drainage divide, m.
- z_r river bed or valley bottom elevation, m.
- z_p peak or ridgetop elevation, m.
- λ wavelength of topography, m.
- ρ_c crustal density, kg/m^3.
- ρ_m mantle density, kg/m^3.

Acknowledgments. I thank Jonathan Stock, Liz Safran, John Buffington, Tim Abbe, and Kevin Schmidt for discussions during the preparation of this study; Tamara Massong for helping to generate Himalayan topographic profiles; and Peter Molnar, Bob Anderson, Philip England, Mike Ellis, and Liz Safran for their critiques of the manuscript. This research was supported by the University of Washington Royalty Research Fund.

References

Amano, K., and A. Taira, Two-phase uplift of higher Himalayas since 17 Ma, *Geology*, *20*, 391-394, 1992.

Axelrod, D. I., Late Tertiary floras and the Sierra Nevadan uplift, *Geol. Soc. Am. Bull.*, *68*, 19–46, 1957.

Banks, R. J., R. L. Parker, and S. P. Huestis, Isostatic compensation on a continental scale: Local versus regional mechanisms, *Geophys. J. R. Astron. Soc.*, *51*, 431–452, 1977.

Bird, P., Initiation of intracontinental subduction in the Himalaya, *J. Geophys. Res.*, *83*, 4975–4987, 1978.

Cervany, P. F., N. D. Naeser, P. K. Zeitler, C. W. Naeser, and N. M. Johnson, History of uplift and relief of the Himalaya during the past 18 million years: Evidence from fission-track ages of detrital zircons from sandstones of the Siwalik Group, in *New Perspectives in Basin Analysis*, edited by K. L. Kleinspehn and C. Paola, pp. 43–61, Springer-Verlag, New York, 1988.

Chase, C. G., and T. C. Wallace, Uplift of the Sierra Nevada of California, *Geology*, *14*, 730–733, 1986.

Christensen, M. N., Late Cenozoic crustal movements in the Sierra Nevada of California, *Geol. Soc. Am. Bull.*, *77*, 163–182, 1966.

Copeland, P., and T. M. Harrison, Episodic rapid uplift in the Himalaya revealed by $^{40}Ar/^{39}Ar$ analysis of detrital K-feldspar and muscovite, Bangal Fan, *Geology*, *18*, 354–357, 1990.

Cotton, C. A., The longitudinal profiles of glaciated valleys, *J. Geology*, *49*, 113–128, 1941.

Dunne, T., and L. B. Leopold, *Water in Environmental Planning*, 818 pp., W. H. Freeman, New York, 1978.

England, P., and P. Molnar, Surface uplift, uplift of rocks, and exhumation of rocks, *Geology*, *18*, 1173–1177, 1990.

Forsyth, D. W., Subsurface loading and estimates of the flexural rigidity of continental lithosphere, *J. Geophys. Res.*, *90*, 12,623–12,632, 1985.

Gilchrist, A. R., and M. A. Summerfield, Differential denudation and flexural isostasy in formation of riftedd-margin upwarps, *Nature*, *346*, 739–742, 1990.

Harrison, T. M., P. Copeland, W. S. F. Kidd, and A. Yin, Raising Tibet, *Science*, *255*, 1663–1670, 1992.

Holmes, A., *Principles of Physical Geology*, 532 pp., Ronald Press, New York, 1945.

Hubbard, M., L. Roden, and K. Hodges, Constraints on unroofing rates in the high Himalaya, eastern Nepal, *Tectonics*, *10*, 287–298, 1991.

Huber, N. K., Amount and timing of late Cenozoic uplift and tilt of the central Sierra Nevada, California—Evidence from the upper San Joaquin River basin, *U.S. Geol. Surv. Prof. Pap. 1197*, 28 pp., 1981.

Huber, N. K., The late Cenozoic evolution of the Tuolumne River, central Sierra Nevada, California, *Geol. Soc. Am. Bull.*, *102*, 102–115, 1990.

Hudson, F. S., Post-Pliocene uplift of the Sierra Nevada, California, *Geol. Soc. Am. Bull.*, *71*, 1547–1574, 1960.

Kirkby, M. J., Hillslope process-response models based on the continuity equation, *Inst. Br. Geogr. Spec. Publ. 3*, 15–30, 1971.

Le Conte, J., Post-Tertiary elevation of the Sierra Nevada shown by the river beds, *Am. J. Sci.*, *19*, 176–190, 1886.

Lyon-Caen, H., and P. Molnar, Constraints on the structure of the Himalaya from an analysis of gravity anomolies and a flexural model of the lithosphere, *J. Geophys. Res.*, *88*, 8171–8191, 1983.

Mathes, F. E., Geologic history of the Yosemite Valley, *U.S. Geol. Surv. Prof. Pap.*, *160*, 137 pp., 1930.

McNutt, M., and H. W. Menard, Lithospheric fluxure and uplifted atolls, *J. Geophys. Res.*, *83*, 1206–1212, 1978.

Mercier, J. L., R. Armijo, P. Tapponnier, E. Carey-Gailhardis, and H. T. Lin, Change from late Tertiary compression to Quaternary extension in southern Tibet during the India-Asia collision, *Tectonics*, *6*, 275–304, 1987.

Molnar, P., and P. England, Late Cenozoic uplift of mountain ranges and global climate change: Chicken or egg?, *Nature*, *346*, 29–34, 1990.

Molnar, P., and P. Tapponnier, Cenozoic tectonics of Asia: Effects of a continental collision, *Science*, *189*, 419–426, 1975.

Montgomery, D. R., and W. E. Dietrich, Channel initiation and the problem of landscape scale, *Science*, *255*, 826–830, 1992.

Nansen, F., The Earth's crust, its surface-forms and isostatic adjustment, *Nor. Vidensk. Akad. Oslo Natur*, *12*, 1–21, 1928.

Pan, Y., and W. S. F. Kidd, Nyainqentanglha shear zone: A late Miocene extensional detachment in the southern Tibetan Plateau, *Geology*, *20*, 775–778, 1992.

Raymo, M. E., and W. R. Ruddiman, Tectonic forcing of the late Cenozoic climate, *Nature*, *359*, 117–122, 1992.

Schmidt, K. M., and D. R. Montgomery, Mountain-scale strength properties, deep-seated landsliding, and limits to local relief, *Eos Trans. AGU*, *73*(43), 227–228, 1992.

Seidl, M. A., and W. E. Dietrich, The problem of channel erosion into bedrock, *Catena Suppl.*, *23*, 101–124, 1992.

Stephenson, R., Flexural models of continental lithosphere based on the long-term erosional decay of topography, *Geophys. J. R. Astron. Soc.*, *77*, 385–413, 1984.

ten Brink, U., and T. Stern, Rift flank uplifts and hinterland basins: Comparison of the Transantarctic Mountains with the Great Escarpment of southern Africa, *J. Geophys. Res.*, *97*, 569–585, 1992.

Turcotte, D. L., and G. Schubert, *Geodynamics: Applications of Continuum Physics to Geological Problems*, 450 pp., John Wiley, New York, 1982.

Unruh, J. R., The uplift of the Sierra Nevada and implications for late Cenozoic epeirogeny in the western Cordillera, *Geol. Soc. Am. Bull.*, *103*, 1395–1404, 1991.

Wager, L. R., The rise of the Himalaya, *Nature*, *132*, 28, 1933.

Wager, L. R., The Arun River drainage pattern and the rise of the Himalaya, *Geogr. J.*, *89*, 239–250, 1937.

Wahrhaftig, C., Stepped topography of the southern Sierra Nevada, California, *Geol. Soc. Am. Bull.*, *76*, 1165–1190, 1965.

Walcott, R. I., Flexural rigidity, thickness, and viscosity of the lithosphere, *J. Geophys. Res.*, *75*, 3941–3955, 1970.

Weissel, J. K., and G. D. Karner, Flexural uplift of rift flanks due to mechanical unloading of the lithosphere during extension, *J. Geophys. Res.*, *94*, 13,919–13,950, 1989.

D. R. Montgomery, Quaternary Research Center, University of Washington, AK-60, Seattle, WA 98195.

(Received March 30, 1993; revised November 2, 1993; accepted January 13, 1994.)